

Supplementary figures:

Fig. S1. Human genes highly correlated with HPV transcript levels are the most differentially expressed between HPV-positive and HPV-negative tumors.

Fig. S2. Transcriptome differences between HPV+ C1 and HPV+ C2 groups.

Fig. S3. E1^{E4} expression levels detected by RNASeq and qPCR are highly correlated.

Fig. S4. Mutation profiles of HPV+ C1 and C2 tumors are not significantly distinct.

Fig. S5. Expression of 582 HPV-correlated genes in JHU OPSCC and TCGA CESCC cohorts.

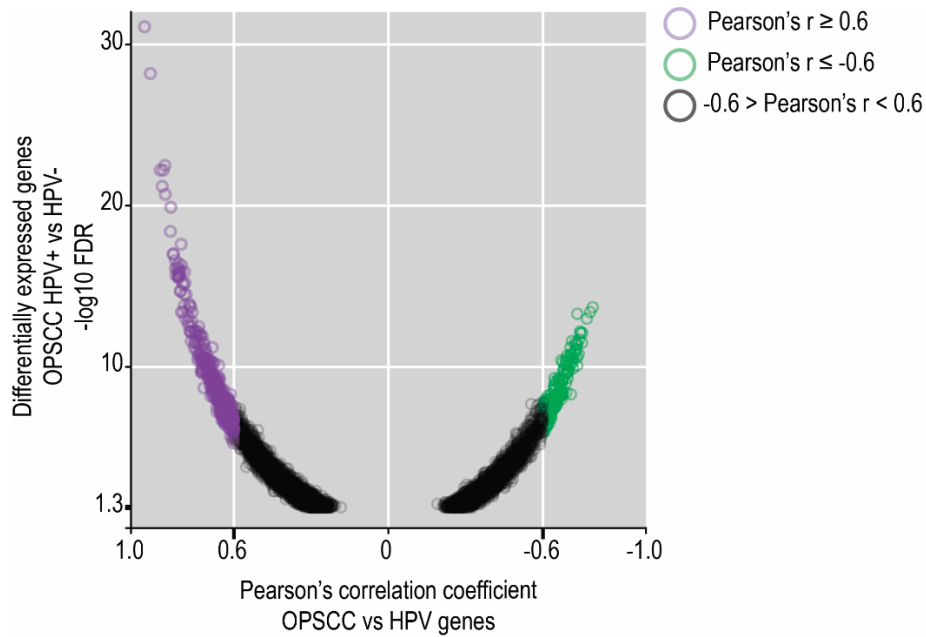


Fig. S1. Human genes highly correlated with HPV transcript levels are the most differentially expressed between HPV-positive and HPV-negative tumors. Distribution of differentially expressed genes between HPV-positive (n=52) and -negative (n=28) OPSCC cases from TCGA according to their FDR ($-\log_{10}$) values (vertical-axis) and their corresponding Pearson correlation coefficient (horizontal-axis) obtained from their correlation with HPV transcripts. Human genes highly correlated with HPV transcription (n=582) (red and green circles) were also highly differentially expressed between HPV-positive and -negative tumors.

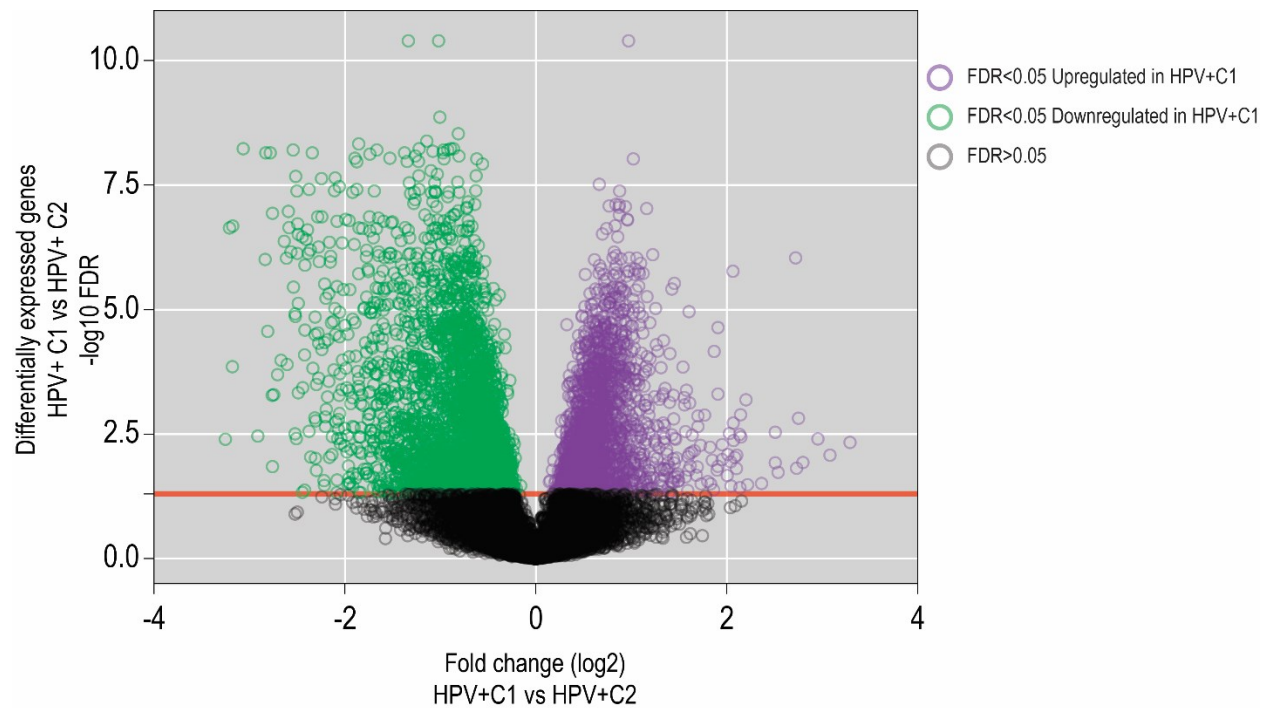


Fig. S2. Transcriptome differences between HPV+ C1 and HPV+ C2 groups. Volcano plot representing \log_2FC (horizontal-axis) and $-\log_{10}FDR$ (vertical-axis) from 20081 genes whose expression was compared between TCGA HPV+ C1 (n=19) and HPV+ C2 (n=33) groups. The red line indicates the significance cutoff at 1.30104 $-\log_{10}FDR$ (FDR=0.05). Among the 5482 differentially expressed genes, 3037 were downregulated and 2445 upregulated in HPV+ C1 cases.

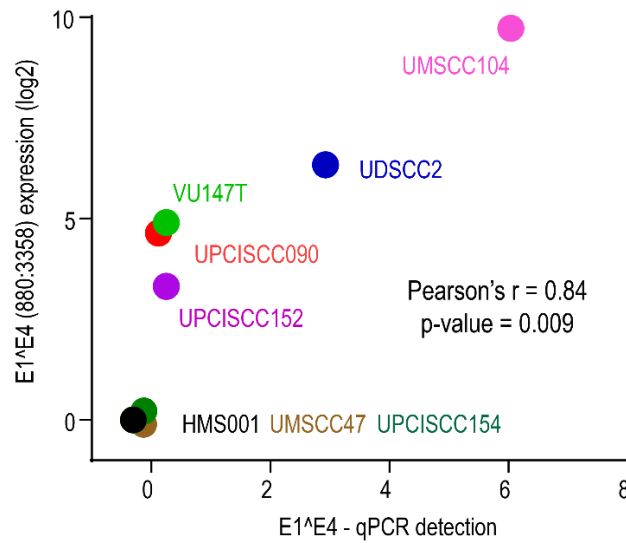


Fig. S3. Levels of E1^{E4} expression detected by RNASeq and qPCR are highly correlated. Correlation between levels of E1^{E4} detected by RNASeq and by qPCR among HPV-positive head and neck cancer cell lines (n=8). Log₂ expression values determined by RNASeq analysis (vertical-axis) were compared to relative expression of E1^{E4} determined by qPCR (horizontal-axis). Absence of E1^{E4} expression in HMS001, UMSCC47, and UPCISCC154 cells was confirmed by both methods. A highly positive correlation (Pearson's correlation coefficient = 0.84) was detected for the two approaches, providing a technical validation of *in silico* findings.

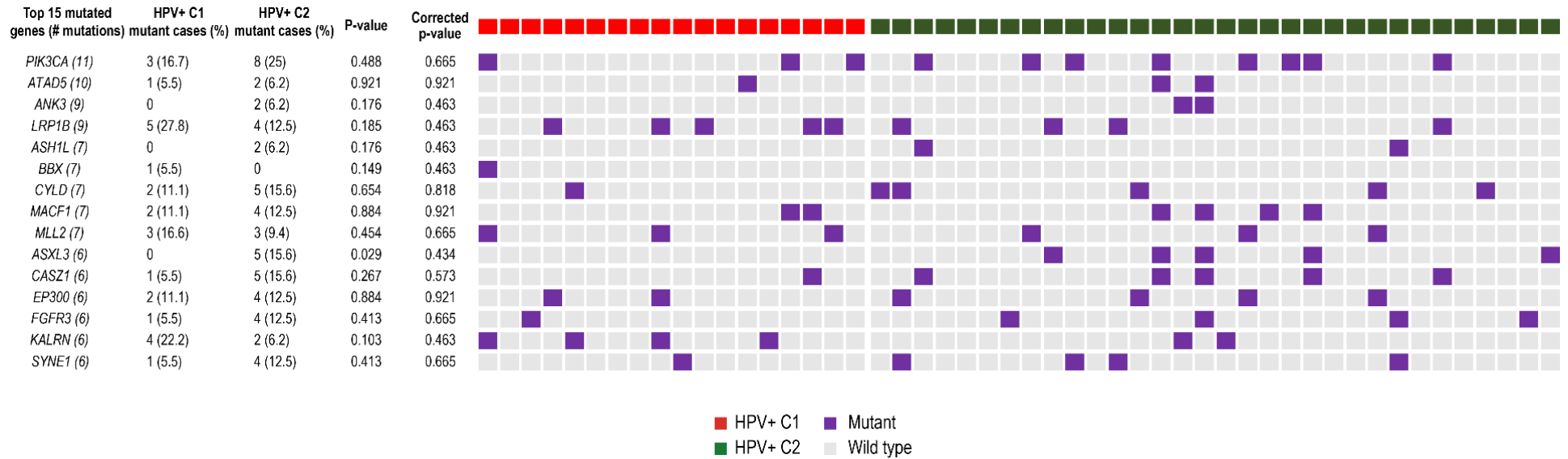


Fig. S4. Mutation profiles of HPV+ C1 and HPV+ C2 tumors are not significantly distinct. The mutation map shows the most common 15 mutated genes and their status among HPV+ C1 (n=19) and HPV+ C2 (n=33) groups. No significant mutation enrichment was found in these groups. The *ASXL3* gene was mutated only among patients in the HPV+ C2 group, but this difference was not confirmed as significant after correction for multiple testing (Fisher's exact test $p=0.029$, corrected $p=0.434$). The *TTN*, *MUC16*, *CSMD3*, *DNAH6*, and *DNAH9* genes were highly mutated, but these mutations were excluded since reliability of genetic variation in these genes is uncertain.

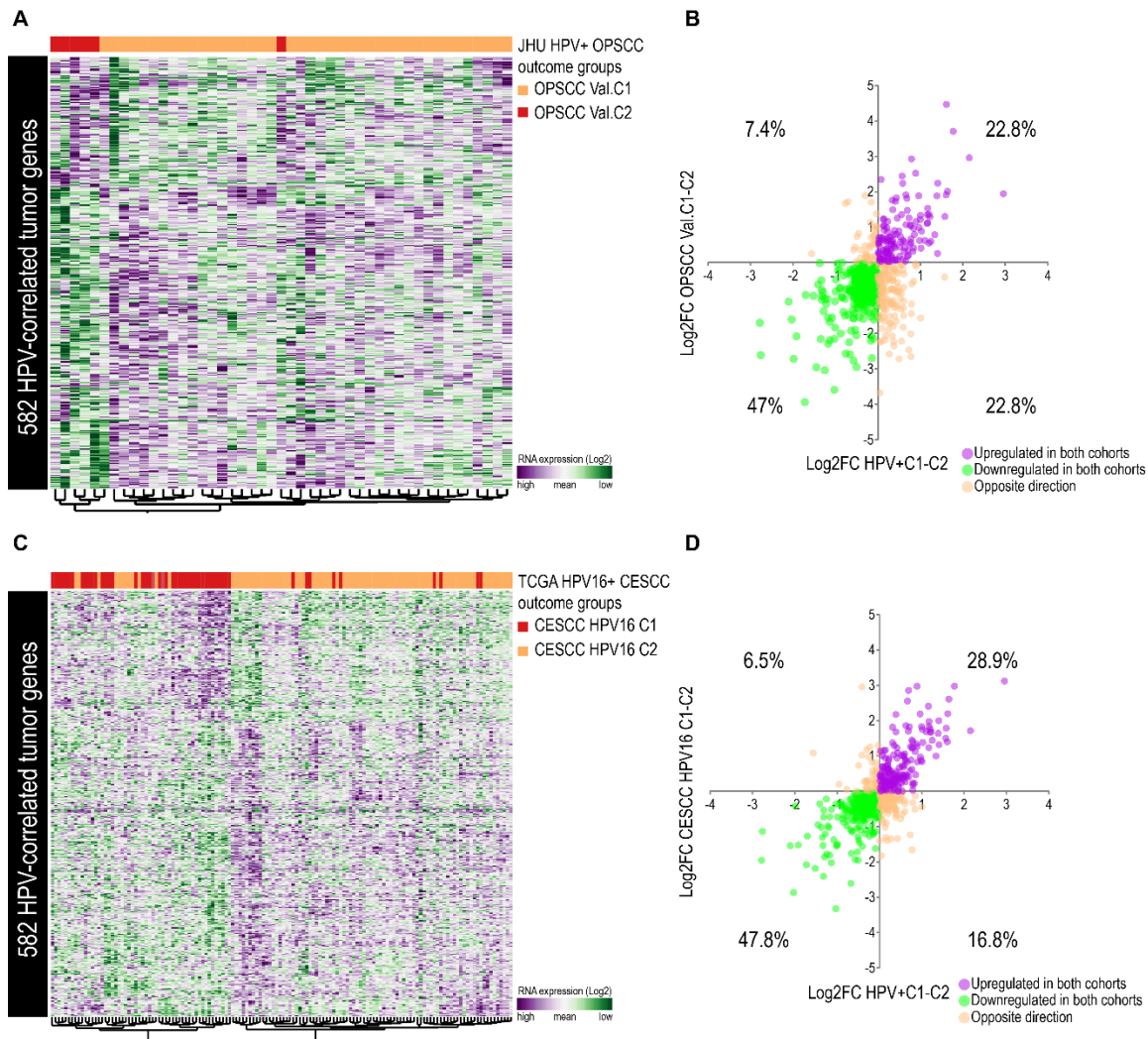


Fig. S5. Expression of 582 HPV-correlated genes in JHU OPSCC and TCGA CESCC cohorts. (A) Expression profile of 582 HPV-correlated genes (vertical-axis) among 47 HPV-positive OPSCC cases from the JHU cohort (horizontal-axis). A tendency toward samples from OPSCC Val.C1 (n=6) clustering together is observed even using the whole set of HPV-correlated genes. **(B)** The expression differences (log₂FC) between HPV+ C1 (n=19) and HPV+ C2 (n=33) groups and between OPSCC Val.C1 (n=6) and Val.C2 (n=33) groups indicate that about 70% of the 582 genes presented the same expression pattern in the poorer prognosis group from each cohort. **(C)** Expression profile of 582 HPV-correlated genes (vertical-axis) among 138 HPV-positive CESCC cases from TCGA (horizontal-axis). A tendency toward CESCC HPV16 C1 (n=50) samples clustering together is observed even using the whole set of HPV-correlated genes. **(D)** About 77% of the 582 genes showed a similar pattern of expression among the poorer prognosis groups from the TCGA OPSCC (n=80) and CESCC (n=138) cohorts.